

Analysis methods

Rohenkohl 2012-

The Journal of Neuroscience

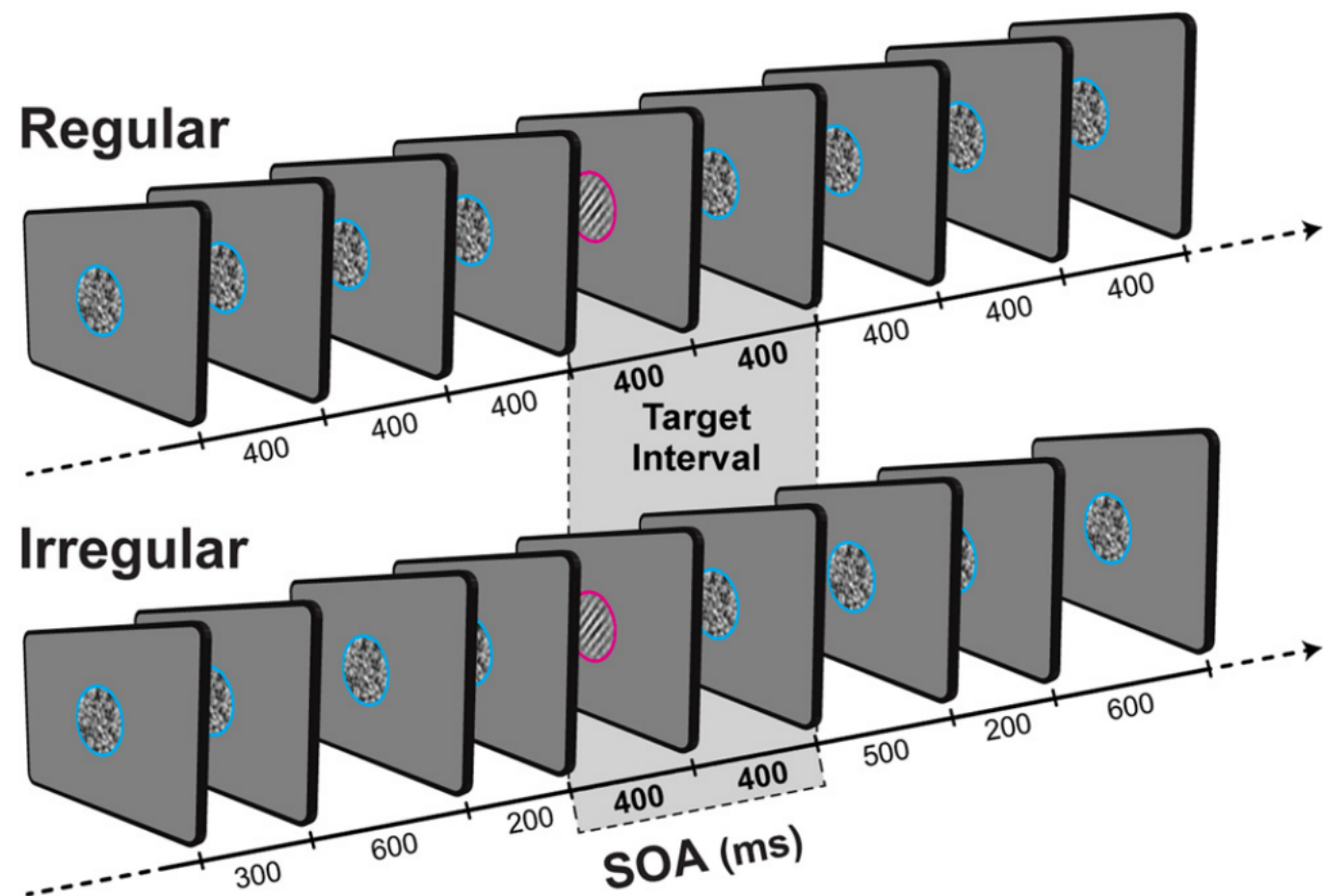


Figure 1. Schematic illustration of the task structure. Each trial consisted of a stream of stimuli presented foveally either with a fixed (regular condition) or jittered (irregular condition) SOA. Notice that the intervals surrounding the targets were exactly the same for the regular and irregular condition. The targets were visual gratings (Gabors) tilted 45° clockwise or counter-clockwise and presented at seven contrast levels to yield a range of performance levels spanning from near chance to near perfect. Participants were asked to respond to the orientation of the target (i.e., left or right) whenever a target was presented. Target presentation was always indicated by a change in the placeholder color to prevent responses to standard stimuli.

Rohenkohl 2012-

The Journal of Neuroscience

- The psychometric data from each participant and condition were fitted with sigmoidal Weibull functions, each defined by three parameters: threshold alpha, slope beta, and fixed lapse-rate gamma (Wichmann and Hill, 2001).
- Guess rates were fixed at 0.5 (i.e., chance level) across all subjects and conditions, and the three parameters were fitted separately for each subject and condition (regular or irregular). Threshold was taken as the predicted contrast level corresponding to 75% accuracy.
- To test for the effect of temporal expectation on target discrimination, fitted threshold and slope values for each participant were submitted to paired t tests. Quality of fit for each subject was assessed by correlating predicted values from the best fitting psychometric function with observed accuracy (mean r-square for group = 0.92, SEM = 0.015; lowest individual r-square = 0.79). The analysis of the psychometric function was performed using the Palamedes toolbox for MATLAB (Prins and Kingdom, 2009).

Rohenkohl 2012-

The Journal of Neuroscience

- The diffusion model (Palmer et al., 2005) predicts that the psychometric function for accuracy $P_C(x)$ and the chronometric function for the mean response time $t_T(x)$ are functions of stimulus strength x according to the two following equations:

$$P_C(x) = \frac{1}{1 + \exp(-kA x)}$$

$$t_T(x) = \frac{A}{kx} \tanh(kA x) + t_R$$

- where k corresponds to the normalized accumulation rate, A to the normalized decision bound, and t_R to the residual time constant. Stimulus strength x follows signal contrast c following a power law whose exponent—which controls the overall slope of both psychometric and chronometric functions as a function of signal contrast—was determined empirically by maximum-likelihood estimation (see below, best-fitting value = 1.97) and fixed across all subjects and conditions.

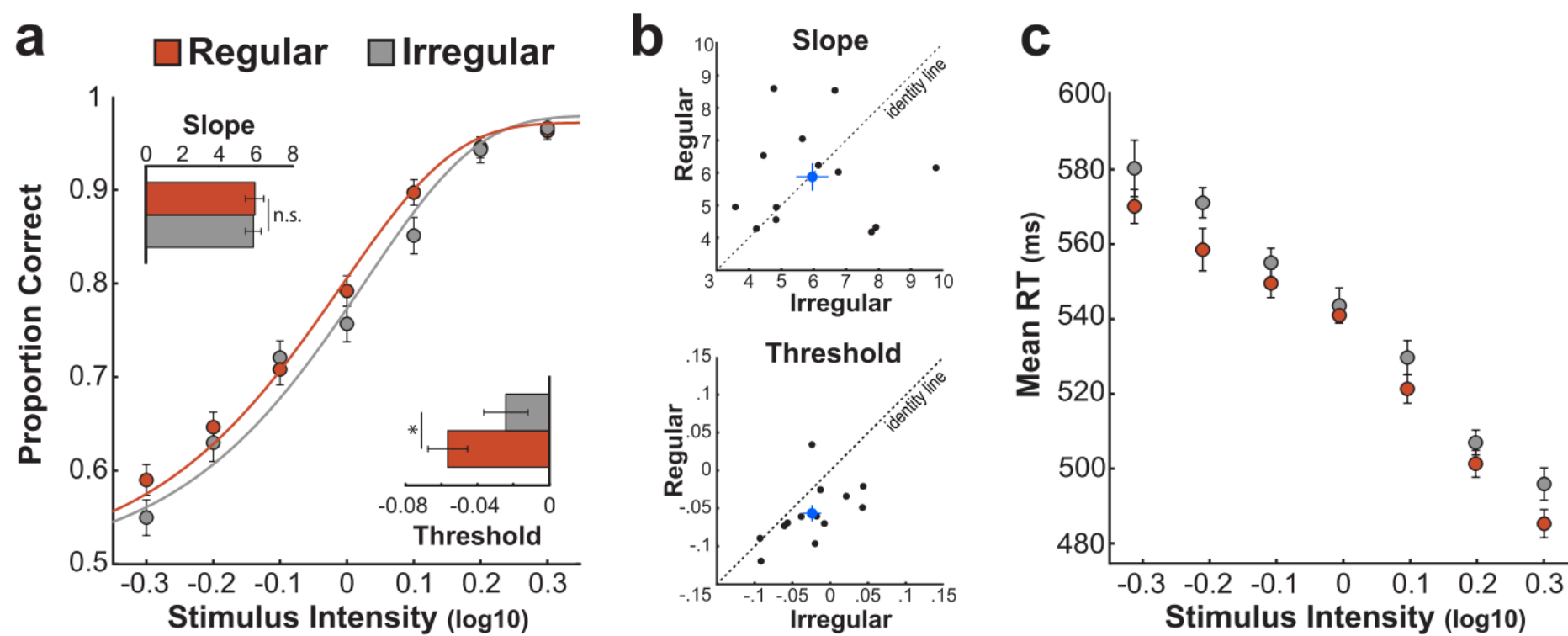
Rohenkohl 2012-

The Journal of Neuroscience

- We performed constrained maximum-likelihood estimation to recover the best-fitting parameter changes for explaining the effect of temporal expectation (i.e., the difference between regular and irregular conditions) on the group-level psychometric and chronometric functions.
- We used group-level means and standard errors to estimate log-likelihood sums for different sets of parameters, and likelihood-ratio tests to compare between nested models.
- Finally, we computed the model predictions for the effect of temporal expectation on psycho-physical threshold using paired t tests that the observed effect did not differ significantly from model-predicted effects.

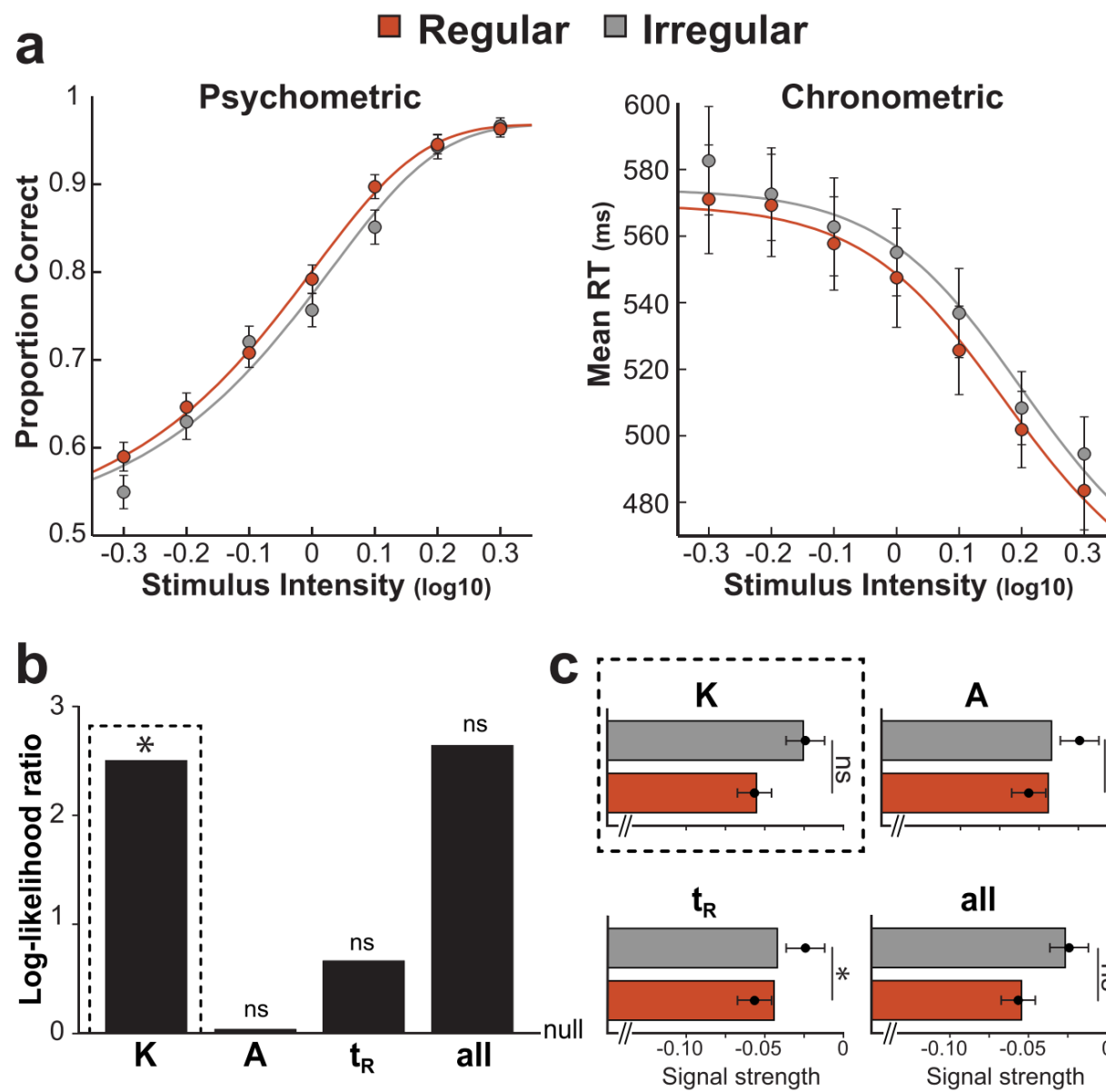
Rohenkohl 2012-

The Journal of Neuroscience



Rohenkohl 2012-

The Journal of Neuroscience



Comparison between behavioral results and diffusion-model predictions. a, Fitted diffusion model to psychometric and chronometric functions at the target contrasts. All three free parameters were fitted separately for the regular (red) and irregular (gray) conditions using maximum-likelihood estimation. b, Hierarchical model comparing tests between nested models to determine which of the three model parameters (the accumulation rate k , the decision-bound A , and the residual time constant t_R) could explain the observed difference between regular and irregular conditions significantly better than a null model for which the three parameters had fixed values across the two conditions. c, Comparison of changes in threshold predicted by each model with the behavioral data. * $p < 0.05$; ns, nonsignificant effect.

Rohenkohl 2014-

Journal of Vision

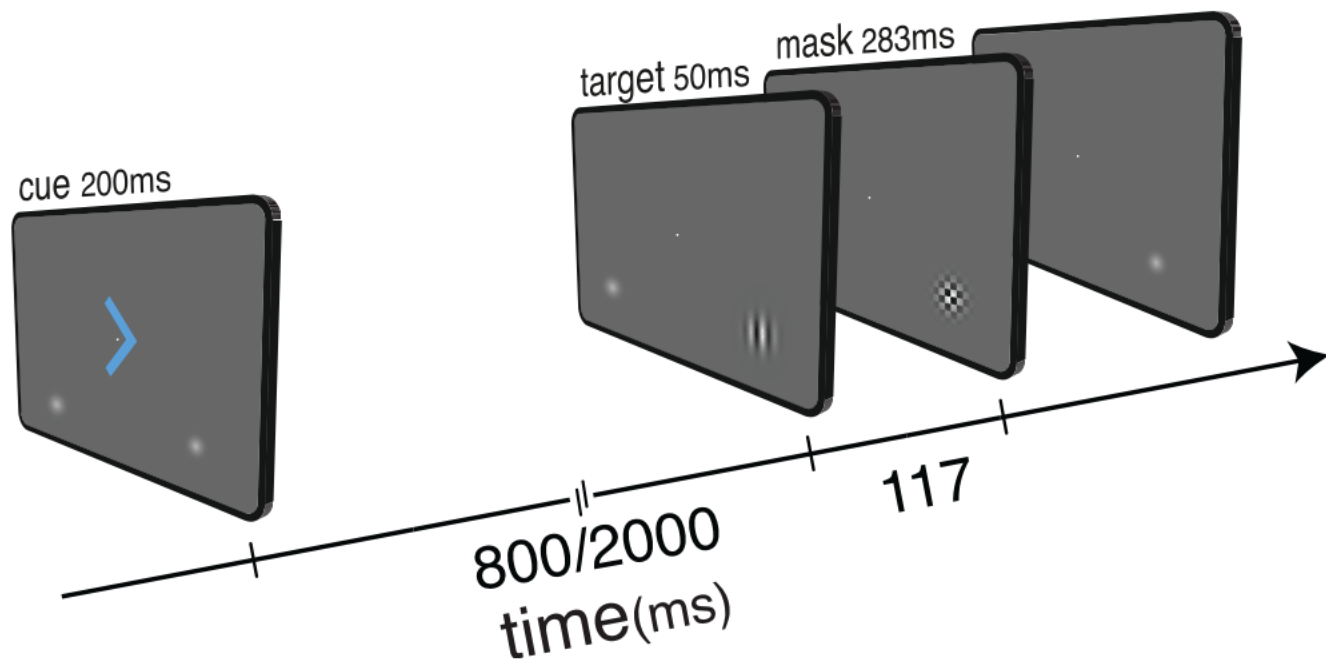


Figure 1. Schematic illustration of the task structure. Foveally presented cues predicted simultaneously where and when target events were more likely to occur. Cue validity for both spatial and temporal expectation was fixed at 80%. Targets consisted of a horizontally or vertically oriented Gabor patch followed by a backward pattern mask. Targets were presented at a fixed contrast, individually adjusted to equate discrimination performance across individuals. Observers responded to the Gabor orientation with their left or right index finger (counterbalanced across subjects).

Rohenkohl 2014-

Journal of Vision

- Statistical analysis was performed using MATLAB and SPSS. Where appropriate, the Greenhouse-Geisser correction for nonsphericity was applied. Saccades were detected using a velocity-based algorithm (Engbert & Mergenthaler, 2006). Trials containing saccades ($>5\%$ trials) were removed from all analyses.
- Behavioral performance was analyzed using perceptual sensitivity values (d'), proportion of correct responses (P_c) and response times. Sensitivity to stimulus orientation was calculated according the formula:
- $d' = z[P_{cH}] + z[P_{cV}]$
- where P_{cH} and P_{cV} correspond to the observers' proportions of correct responses to horizontal and vertical stimuli respectively, and z to the inverse normal (z score) transformation.

Rohenkohl 2014-

Journal of Vision

- Response times were adjusted according to the observers' accuracy in order to account for possible speed-accuracy trade-offs. Similarly to previous studies, this adjustment was done using a measure called inverse efficiency. The inverse efficiency (IE) is calculated by dividing the mean reaction time by the proportion of correct responses.
- Repeated-measures ANOVAs were performed using the Greenhouse-Geisser correction for nonsphericity.
- Additionally, we used nonparametric permutation tests to control for possible biases in the statistics due to difference in power between valid and invalid conditions.

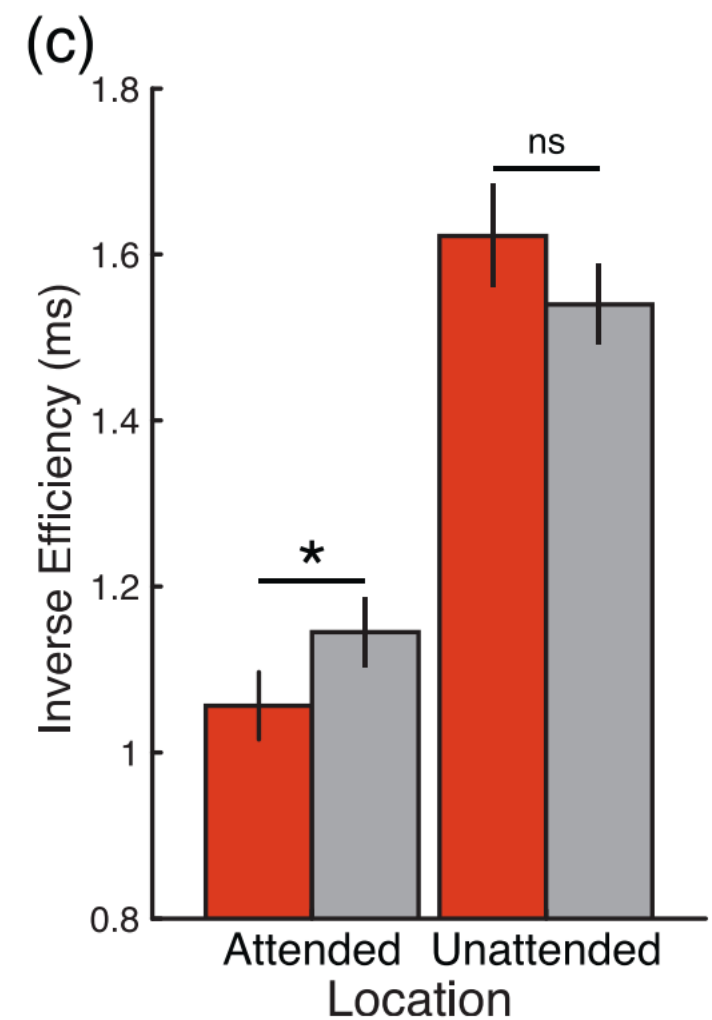
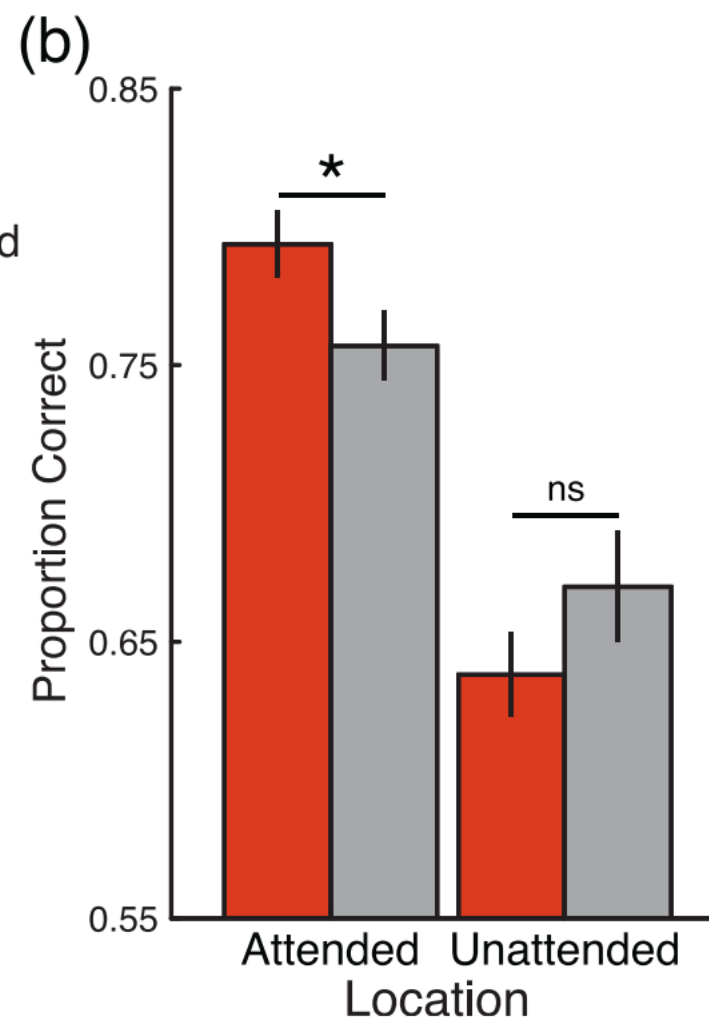
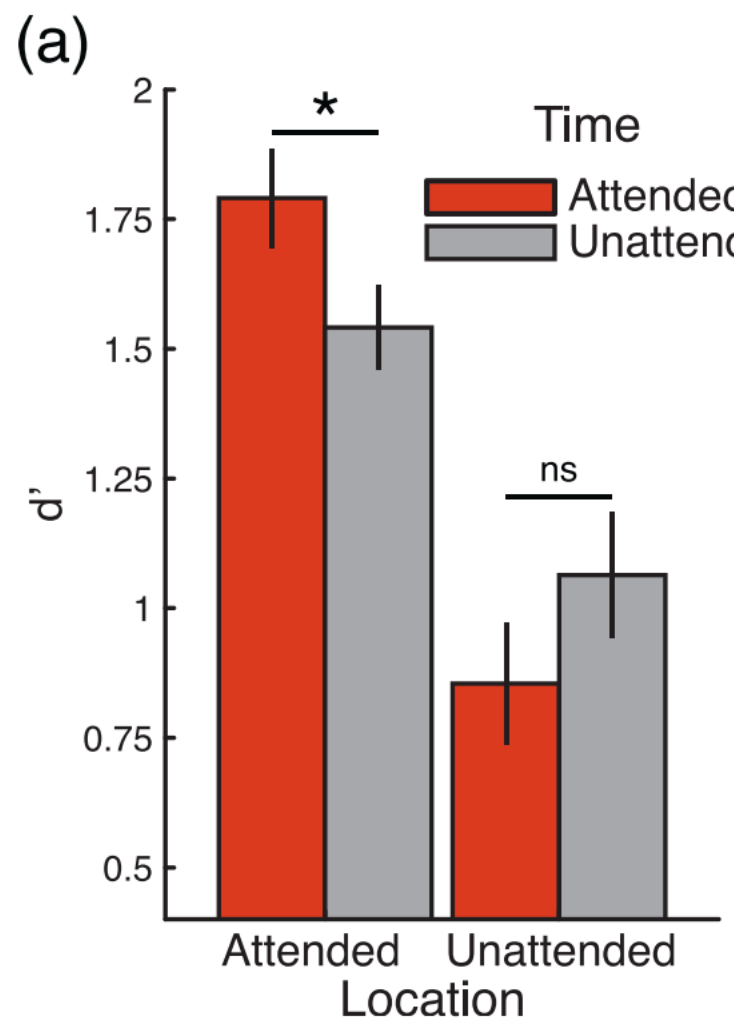
Rohenkohl 2014-

Journal of Vision

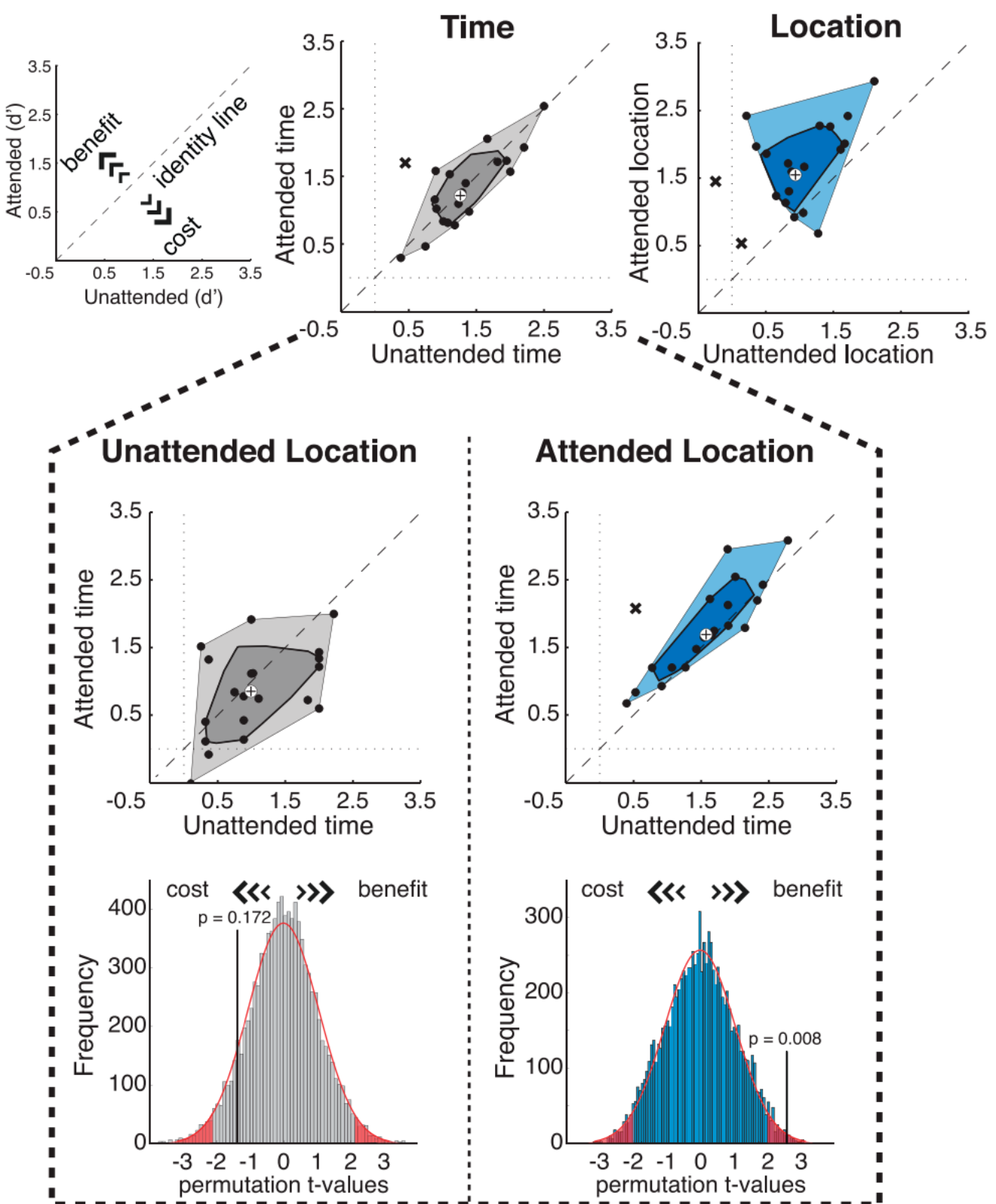
- First, we calculated the mean difference between conditions of interest for each participant. We then performed F tests (ANOVAs) or t tests (for post-hoc comparisons) on these values. Both statistical tests were two-sided and used a critical alpha level of 0.05. We assessed the significance of the observed results by comparison to a null distribution generated via Monte Carlo simulation with 10,000 repetitions.
- This null distribution was generated by randomly shuffling the condition labels within each participant's data in each repetition.
- We then performed the statistical test (F or t tests) on the mean difference between the conditions of interest, and the resulting value was entered into the null distribution.
- The permutation p value was determined as the proportion of random partitions that resulted in a larger test statistic than the observed one.

Rohenkohl 2014-

Journal of Vision



Effects of temporal expectations on d' measures at the individual level and permutation tests. Scatter and bagplots showing the main effects of temporal and spatial expectations (Top) and the effect of temporal expectation at the attended and unattended locations (Bottom). Blue indicates the conditions in which there was a significant effect of expectation. The cross at the center of the bagplot represents the center of mass of the bivariate distribution of empirical data, the darker area includes 50% of the data with the largest depth, the lighter polygon contains all other nonoutlier data points, and the Xs represent outliers (Rousseeuw, Ruts, & Tukey, 1999). Outliers were detected using the “Skewness-Adjusted Outlyingness” method using LIBRA toolbox for MATLAB (Verboven & Hubert, 2005; for more details on this method see Hubert & Van der Veeken, 2008). Histograms showing the distributions generated from 10,000 random permutations from data sets of 20 participants (see Methods for details). Original t test values (Attended vs. Unattended time at Unattended (left) and Attended (right) Locations) are indicated by the black vertical lines



Samaha 2015-

PNAS

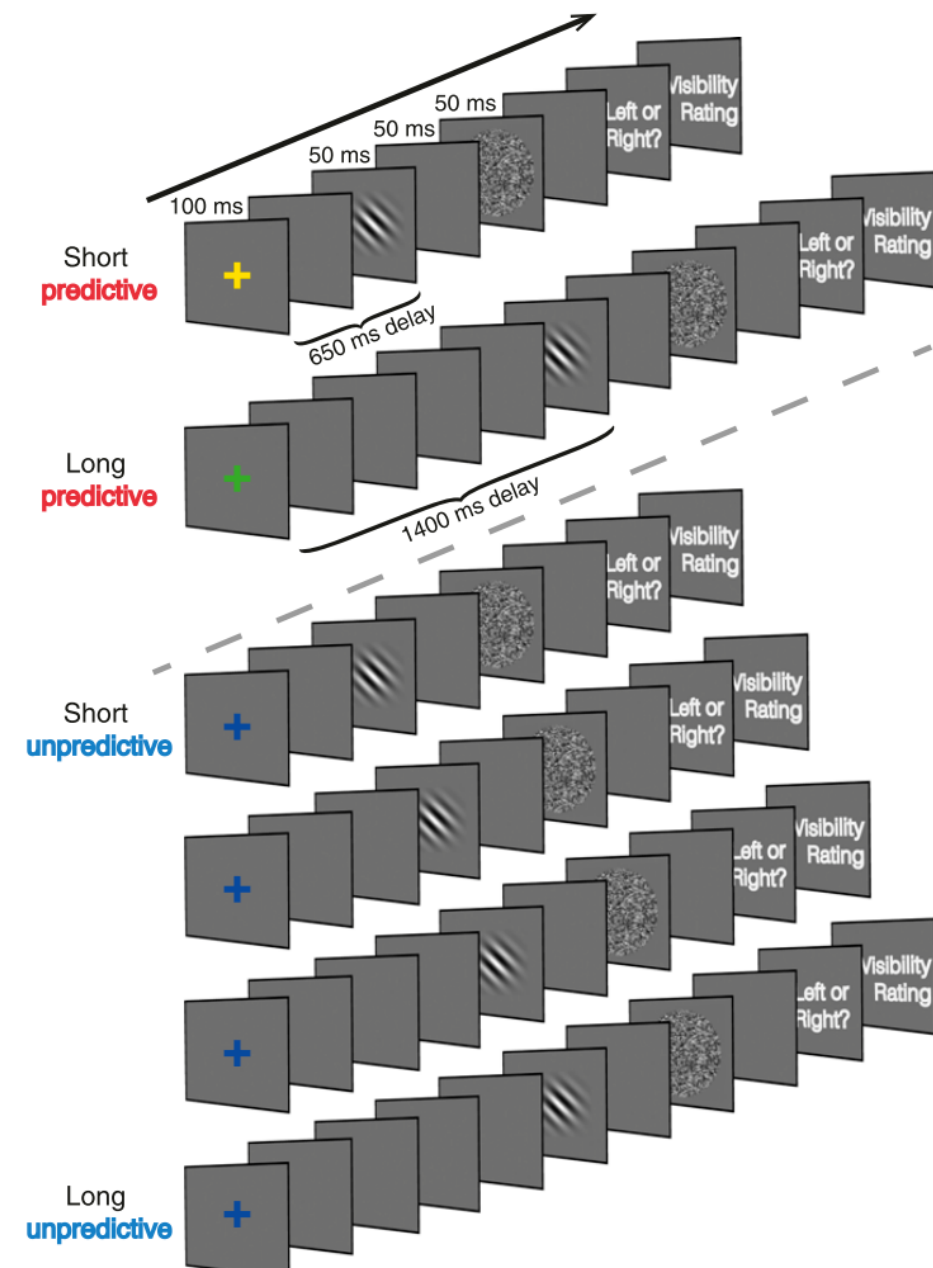


Fig. 1. Schematic of trial types and timing. Colored fixation crosses cued the appearance of target Gabor patches at a short, long, or unpredictable delay (a random selection of one of four delays). Participants provided nonspeeded, two-alternative forced-choice (2AFC) orientation judgments, followed by a seen or guess judgment (experiment 1) or using the perceptual awareness scale (experiment 2).

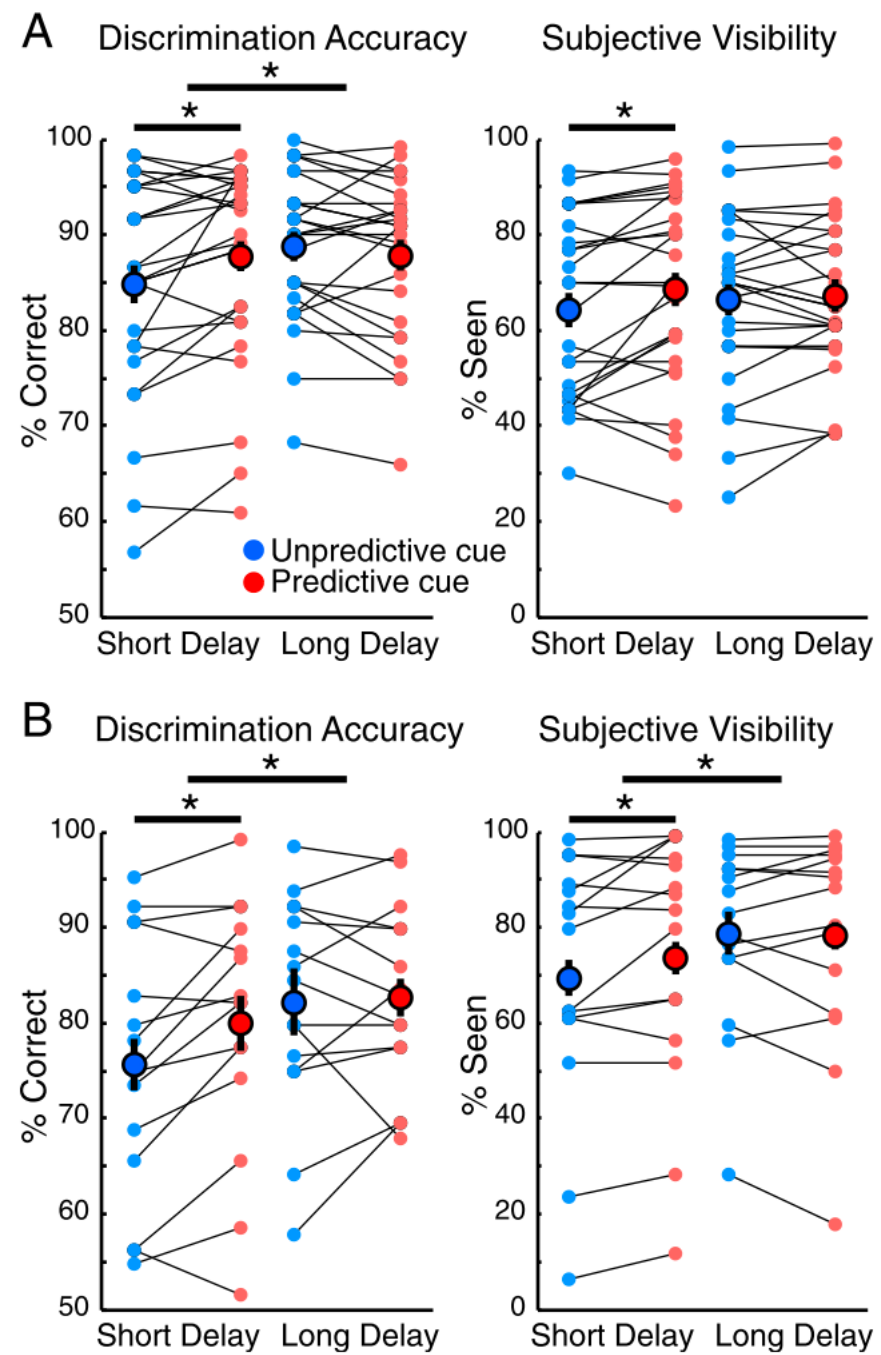
Samaha 2015-

PNAS

- Accuracy and subjective visibility data from experiment 1 were each submitted to a repeated-measures ANOVA with delay (short, long) and cue type (predictive, unpredictive) as within-subject factors.

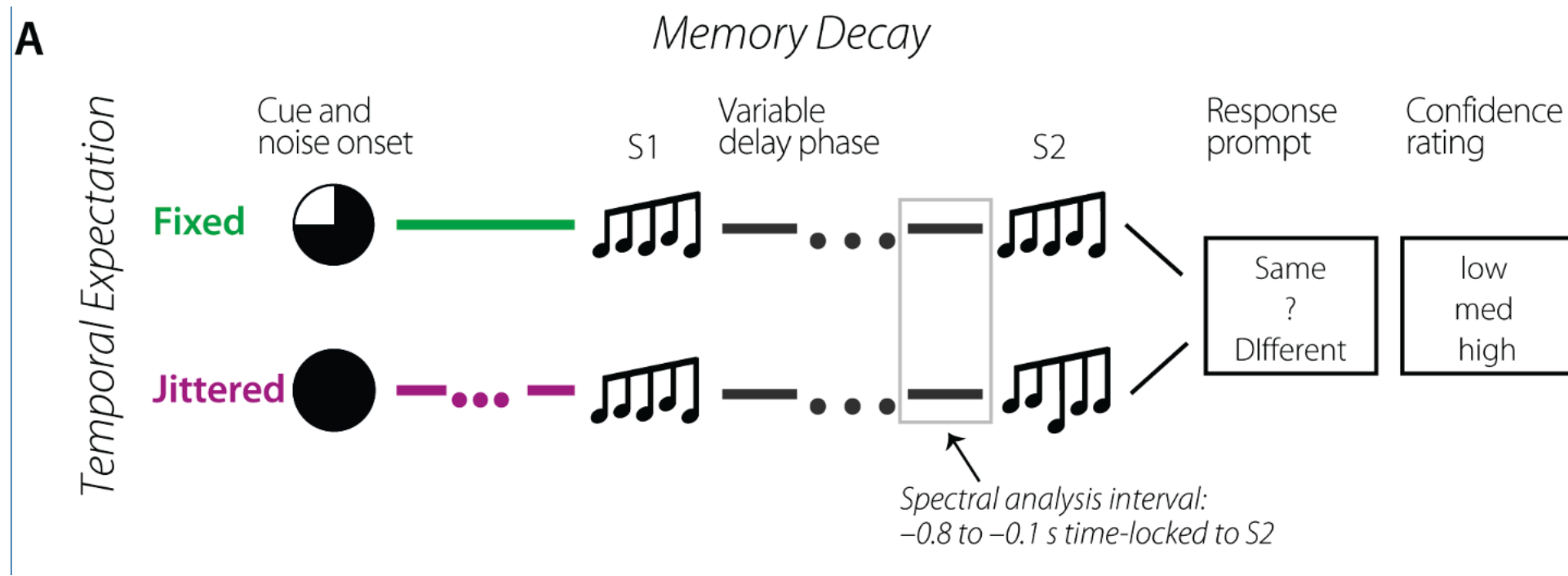
Samaha 2015-

PNAS



Wilsch 2018-

The Journal of Neuroscience



- Experimental design and behavioral performance. A. Experimental design. The upper panel illustrates a “same” trial (S1 and S2 are the same) with a fixed onset time. The lower panel illustrates a “different” trial (S1 and S2 are different) with jittered onset time. The actual durations of the variable delay phases are specified in B and D. The light gray box indicates the interval of the spectral analyses: -0.8 to -0.1 s time-locked to S2.

Wilsch 2018-

The Journal of Neuroscience

- The crucial measure for memory decay was the performance measure Az, a non-parametric performance measure derived from confidence ratings.
- Hit and false alarm rates at each confidence level were used to construct receiver operating characteristic (ROC) curves (Macmillan and Creelman, 2004) for each condition, and ROC curves were used to derive Az.
- Az corresponds to the area under the ROC curve and can be interpreted similarly to proportion correct. Az was computed for each of the twelve conditions (temporal expectation, 2, × memory decay, 6), allowing us to estimate memory decay as a function of delay-phase duration separately for fixed and jittered onset times.

Wilsch 2018-

The Journal of Neuroscience

- We fitted Equation 1 (Glass and Mackey, 1988) to Az scores as a function of delay-phase duration:
- $$x(t) = x_0 + e^{-\gamma t} + \frac{\lambda}{\gamma}(1 - e^{-\gamma t}) \quad (1)$$
- where t is equal to time (i.e., delay-phase duration) and x_0 corresponds to the intercept. This specific function contained a term describing decay, γ , and an additional term describing growth, λ . The ratio indicates the function's asymptote.

Wilsch 2018-

The Journal of Neuroscience

- In addition, we also fitted a decay-term-only model (i.e., first term: $x(t) = (x_0 + e^{-\gamma t})$) The decay-only model is more parsimonious and more commonly used to estimate memory decay (Peterson and Peterson, 1959; Wickelgren, 1969).
- To determine which one of these two models represented the memory performance data best, we calculated the Bayesian information criterion (BIC; Schwarz, 1978) for both model fits, as well as for fixed and jittered onset times separately.
- Note that the BIC penalizes for more parameters and allows for an equitable comparison of goodness-of-fit of both models (smaller is better). We averaged the BICs across fixed and jittered onset times separately for each function.

Wilsch 2018-

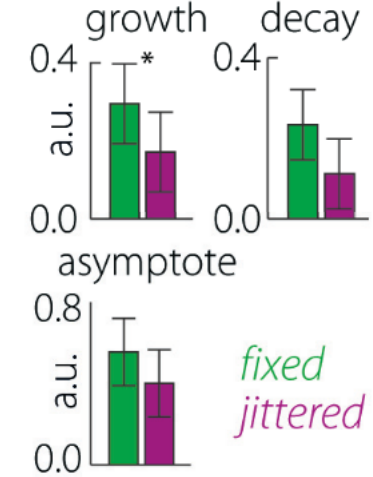
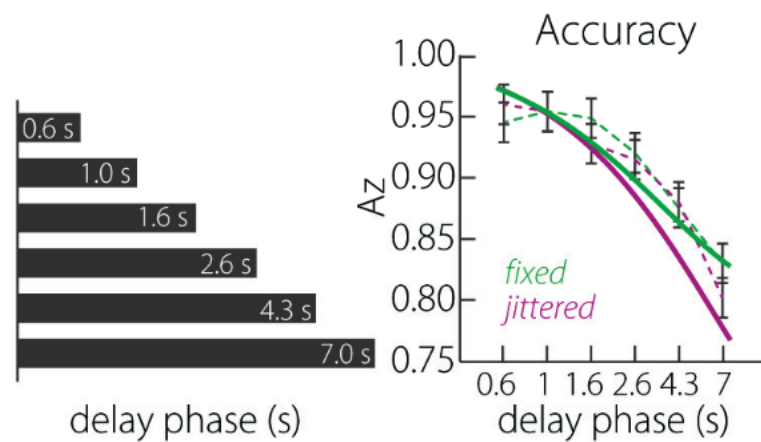
The Journal of Neuroscience

- 17 out of 18 participants had a lower BIC for the full model (Equation 1) than the decay-only model indicating an overall better fit by the former model. Therefore, all further analyses were conducted on the parameters resulting from the fit of the complete Equation 1. Four of the participants were excluded from subsequent analyses, because R^2 , an indicator for goodness of the model fit, of their fitted models was smaller than 0.3 (see Figure 1C for individual model fits). The average R^2 values for the fixed and jittered conditions, respectively, were 0.66.
- After the fitting of the function, the resulting parameters x_0 , gamma, lambda and for jittered and fixed onset times as dependent variables were assessed with a multivariate ANOVA. This allowed us to test whether there is a global difference between jittered and fixed onset times.
- Subsequently, the parameters x_0 , gamma, lambda were tested for differences between fixed and jittered onset times with univariate repeated-measures ANOVAs, to determine whether memory decay was less strong when S1-onset times were predictable

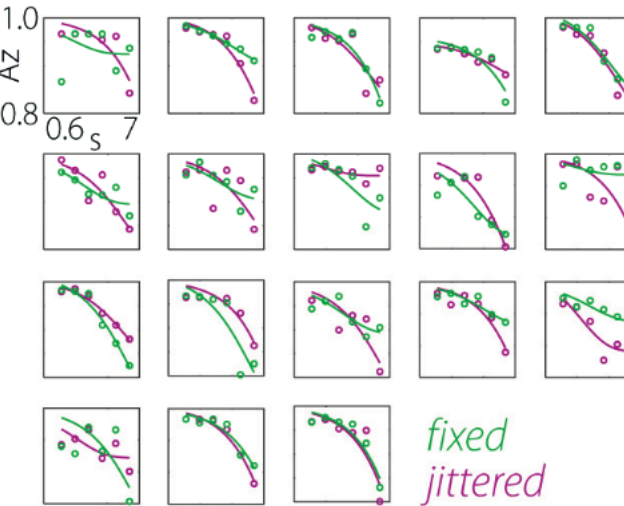
Wilsch 2018-

The Journal of Neuroscience

B



C



Rohenkohl 2011-

PlosOne

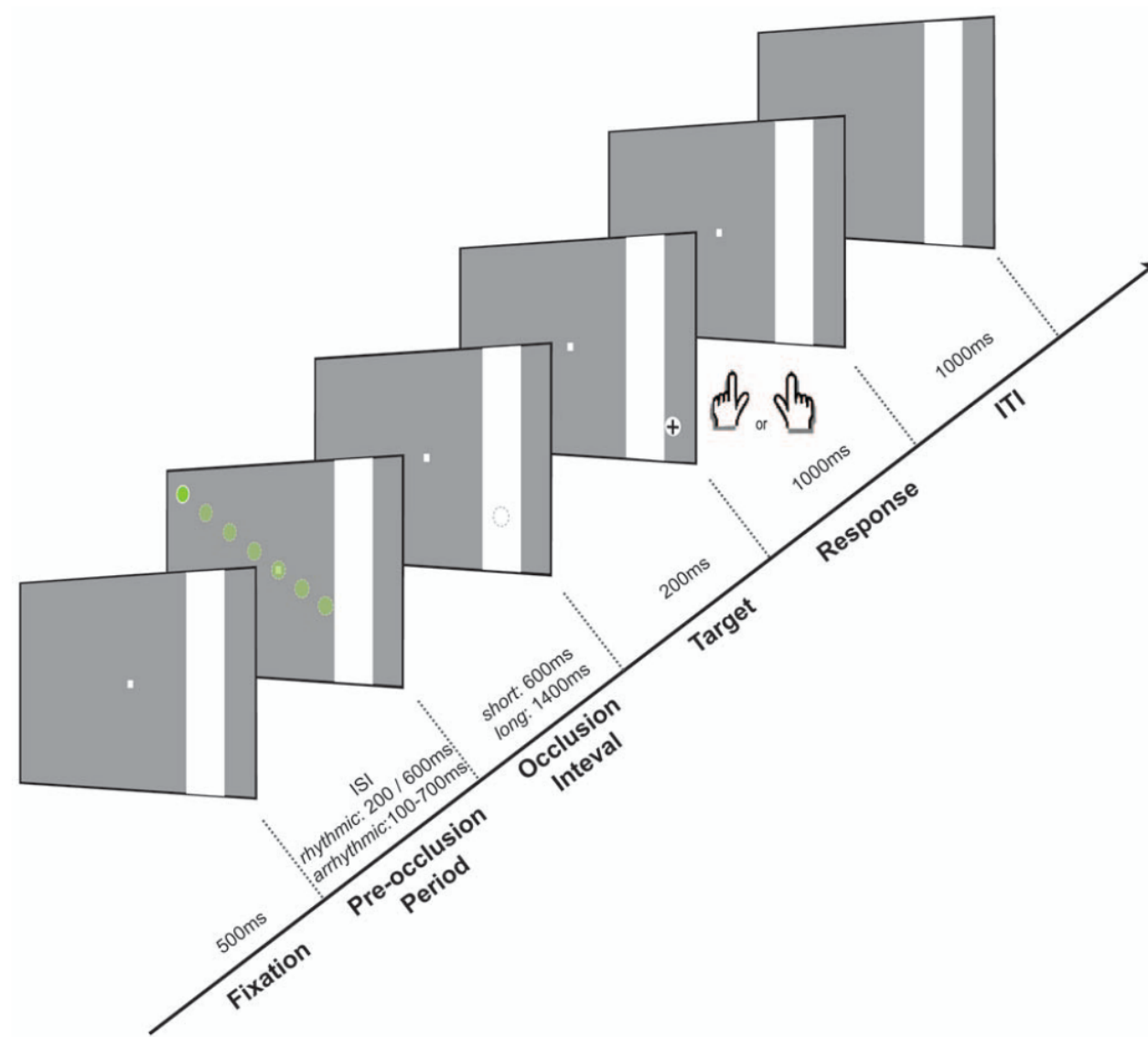
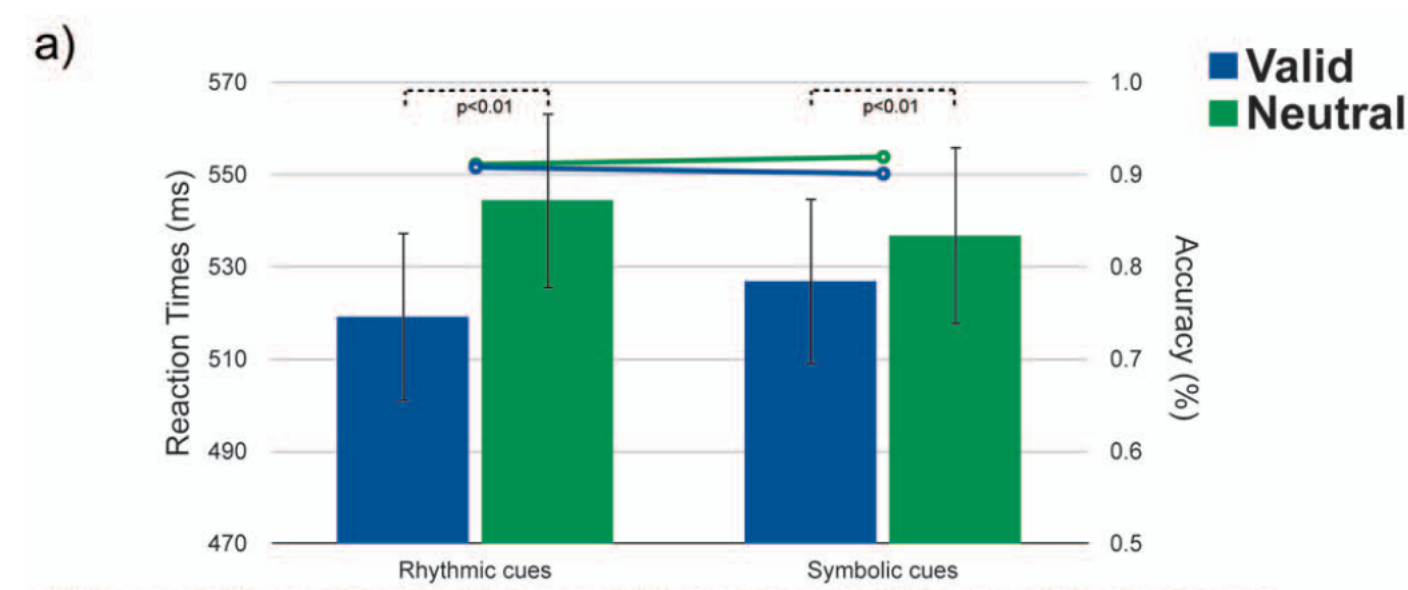
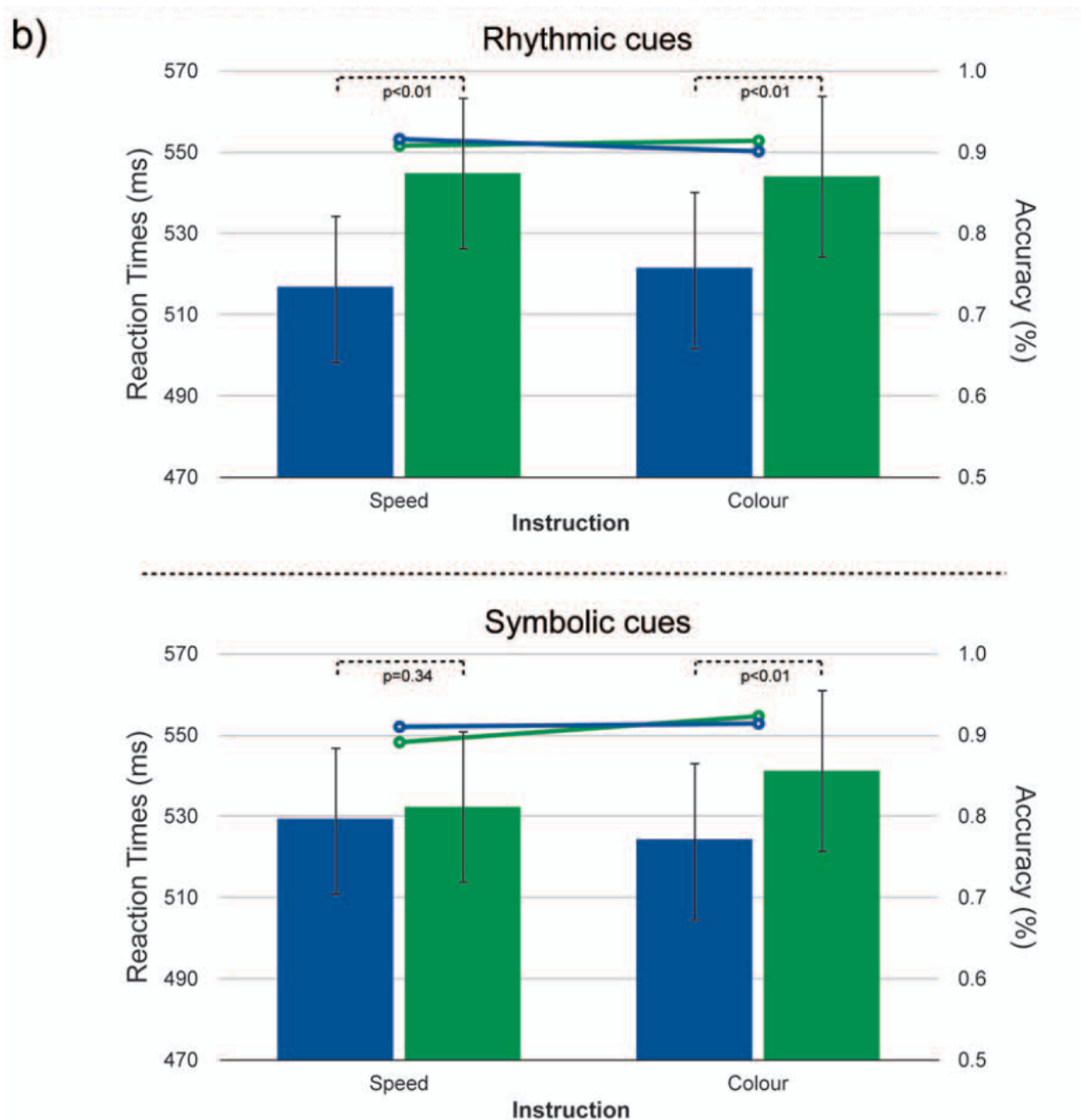


Figure 1. Schematic of the task. A coloured ball appears at the left side of a grey screen and moves across the screen in seven steps. After reaching the occluding band, the ball disappears behind for a single step. When the ball reappears it contains either an upright (50%) or a tilted (50%) cross. Temporal expectations could be induced by the rhythm and/or the colour of the balls preceding the occlusion.
doi:10.1371/journal.pone.0014620.g001

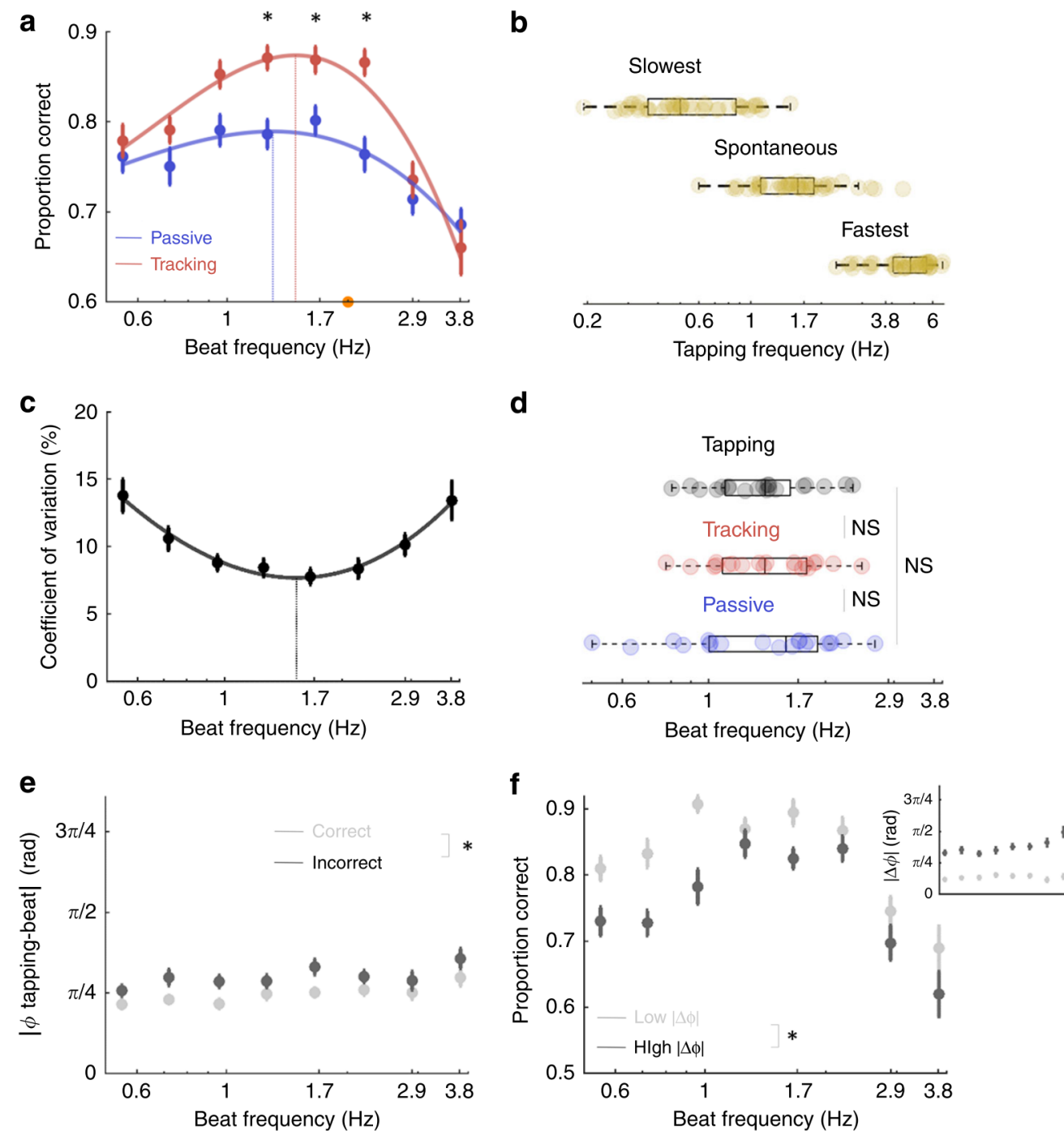
Rohenkohl 2011 -

PlosOne



Zalta 2020-

Nature communication



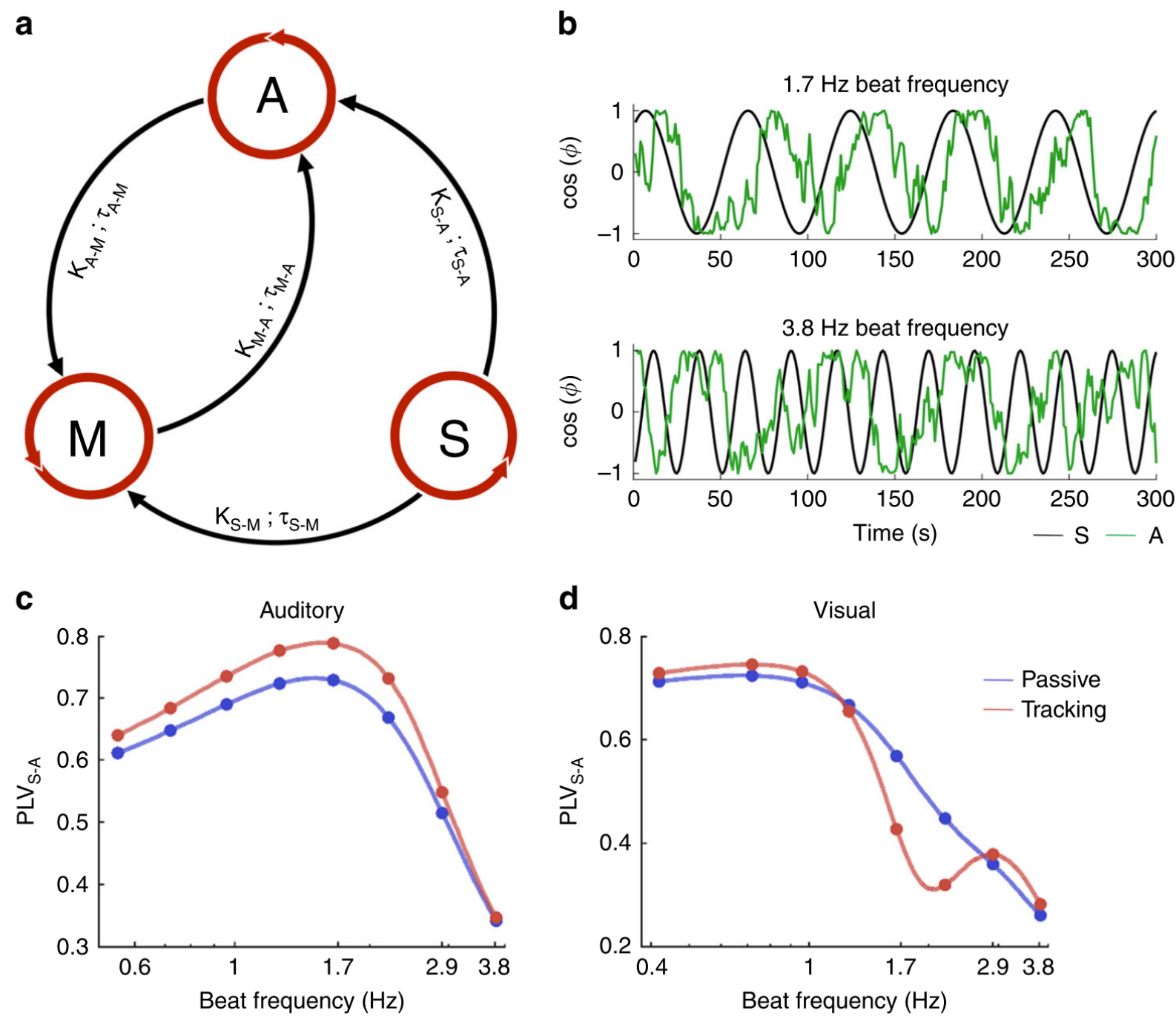
Zalta 2020-

Nature communication

- Fig. 2 Motor contribution to auditory temporal attention and free tapping. a Experiment 2. Average performance per condition (beat frequency) in the passive (blue) and tracking (red) sessions. In the passive session, participants performed the task without moving before the end of the sequence. In the tracking session, participants performed the task while expressing the tempo by moving their index finger. Average performance per condition (beat frequency). Data were approximated with a polynomial function (plain line), and an optimal tempo (leading to a maximal performance) could be estimated (vertical line). The orange dot indicates the tempo (2 Hz) that served to estimate the individual difficulty level. b Free tapping experiment (exp. 3). Individual average frequency of free tapping in three conditions where participants had to rhythmically tap at their slowest, spontaneous and fastest rate. c–f Experiment 2: c Coefficient of variation (CV; i.e., relative standard deviation) of guided tapping across conditions in the tracking session. Same conventions as in a. d Individual estimates of the optimal tempo of auditory temporal attention in the passive (blue) and tracking (red) sessions (from A) and of guided motor tapping in the tracking session (black; from c). e Sensorimotor simultaneity (Φ ; in radian), i.e., temporal distance between motor acts and the beat (in absolute value, normalised to the beat period) across conditions in the tracking session, for correct (light grey) and incorrect (dark grey) trials. f Average performance per condition in the tracking session for trials with low (light grey) and high (dark grey) sensorimotor simultaneity indexes. Trials were sorted according to a median-split procedure. The inset plot indicates the associated sensorimotor simultaneity indexes. Error bars indicate s.e.m. (n = 20; (a) paired t-tests, (e–f) repeated-measures ANOVA; *p < 0.05; NS non-significant). Boxplots represent median and 1.5 times the interquartile range.

Zalta 2020-

Nature communication



Zalta 2020-

Nature communication

- A model of coupled oscillators to generalise the results. a Model of three delay-coupled phase oscillators approximating the selective coupling between the external beat (stimulus S), sensory-specific temporal attention (A), and natural motor dynamics (M). The external oscillator (S) influences attention and motor oscillators with a specific strength K and delay τ , and attention and motor oscillators reciprocally influence each other. The phase-locking value (PLV) between the external beat (S) and the sensory-specific temporal attention oscillator (A) reflects the capacity of A to entrain to S and thus is used as an approximation of behavioural performance. b Example of dynamics of the auditory temporal attention oscillator (A; green) during presentation of an external beat (S; black) at 1.7 Hz or 3.8 Hz. c, d Replication of the (c) auditory (exp. 2) and (d) visual (exp. 5) passive (blue) and tracking (red) experiments. Difference between conditions was obtained by adjusting three key parameters: the natural frequency of the sensory-specific temporal attention oscillator (A) and the time-delay between the stimulus (S) and the motor oscillator (M) which varied across modalities (auditory: $\omega_A = 1.5$ Hz, $\tau_{S-M} = 0.1$ s; visual: $\omega_A = 0.7$ Hz, $\tau_{S-M} = 0.35$ s), and the coupling strength between motor and attention oscillators, which varied between passive ($K_{M-A} = 2$) and tracking ($K_{M-A} = 10$) sessions.

Zalta 2020-

Nature communication

$$\dot{\theta}_S = \omega_S,$$

$$\dot{\theta}_A = \omega_A + K_{AM} \sin[\theta_M(t - \tau_{AM}) - \theta_A] + K_{AS} \sin[\theta_S(t - \tau_{AS}) - \theta_A] + \xi_A(t),$$

$$\dot{\theta}_M = \omega_M + K_{MA} \sin[\theta_A(t - \tau_{MA}) - \theta_M] + K_{MS} \sin[\theta_S(t - \tau_{MS}) - \theta_M] + \xi_M(t),$$

- where ω_i , θ_i and ξ_i are the natural frequency, phase and noise of an oscillator i , and for each pair of oscillators i and j , K_{ij} and τ_{ij} represent the coupling strength and time-delay from oscillator i to j . The noise ξ_i is additive and Gaussian with an intensity D , such as $\langle \xi_i(t) \rangle = 0$ and $\langle \xi_i(t) \xi_j(t') \rangle = 2D_{ij}\delta(t - t')\delta_{ij}$ (where $\langle . \rangle$ denotes the time-average operator and δ the delta function). In line with studies implementing models of coupled oscillators, we ran the simulation during 1e4 seconds, in order to obtain an equilibrium in the interaction between the coupled oscillators^{52,97} and to approximate the duration (summed across trials and participants) of the behavioural experiments. The sampling rate of the simulation was 25 ms. We thus set internal time-delays to 0 ms (i.e., <25 ms).

Zalta 2020-

Nature communication

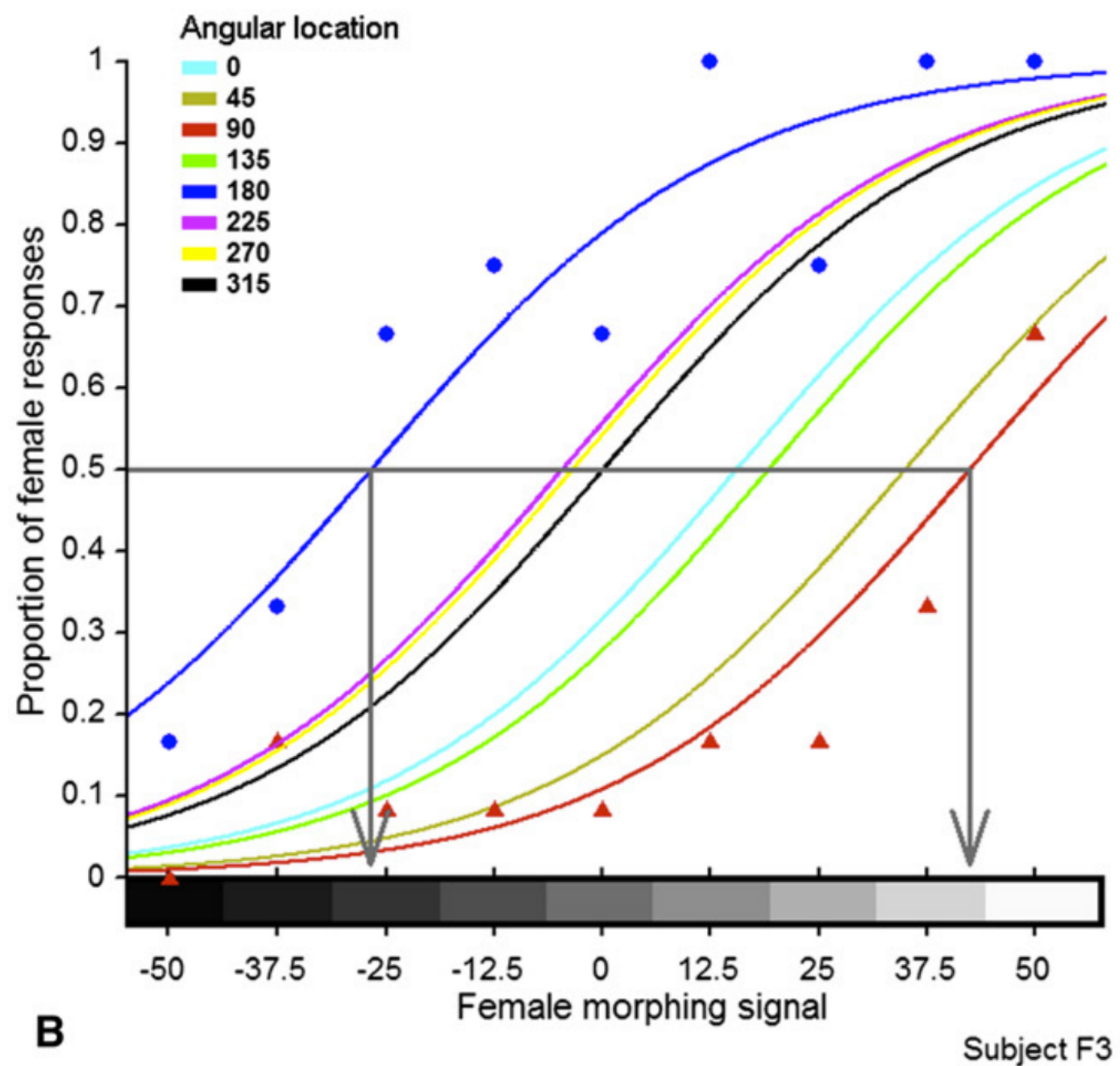
- The level of coherence between the external beat S and the sensory-specific oscillator A was computed with the phase-locking value (PLV)^{52,53}. It estimates the capacity of A to entrain to S and is hence used as an approximation of behavioural performance. PLV is defined as:

$$\text{PLV}_{S-A} = \frac{1}{N} \sum_{t=1}^N e^{i\Delta\theta_{SA}(t)},$$

- where the phase angle $\Delta\theta$ between oscillators S and A at time t is averaged across time points from t=1 to N.

Afraz 2010-

Current Biology



Afraz 2010-

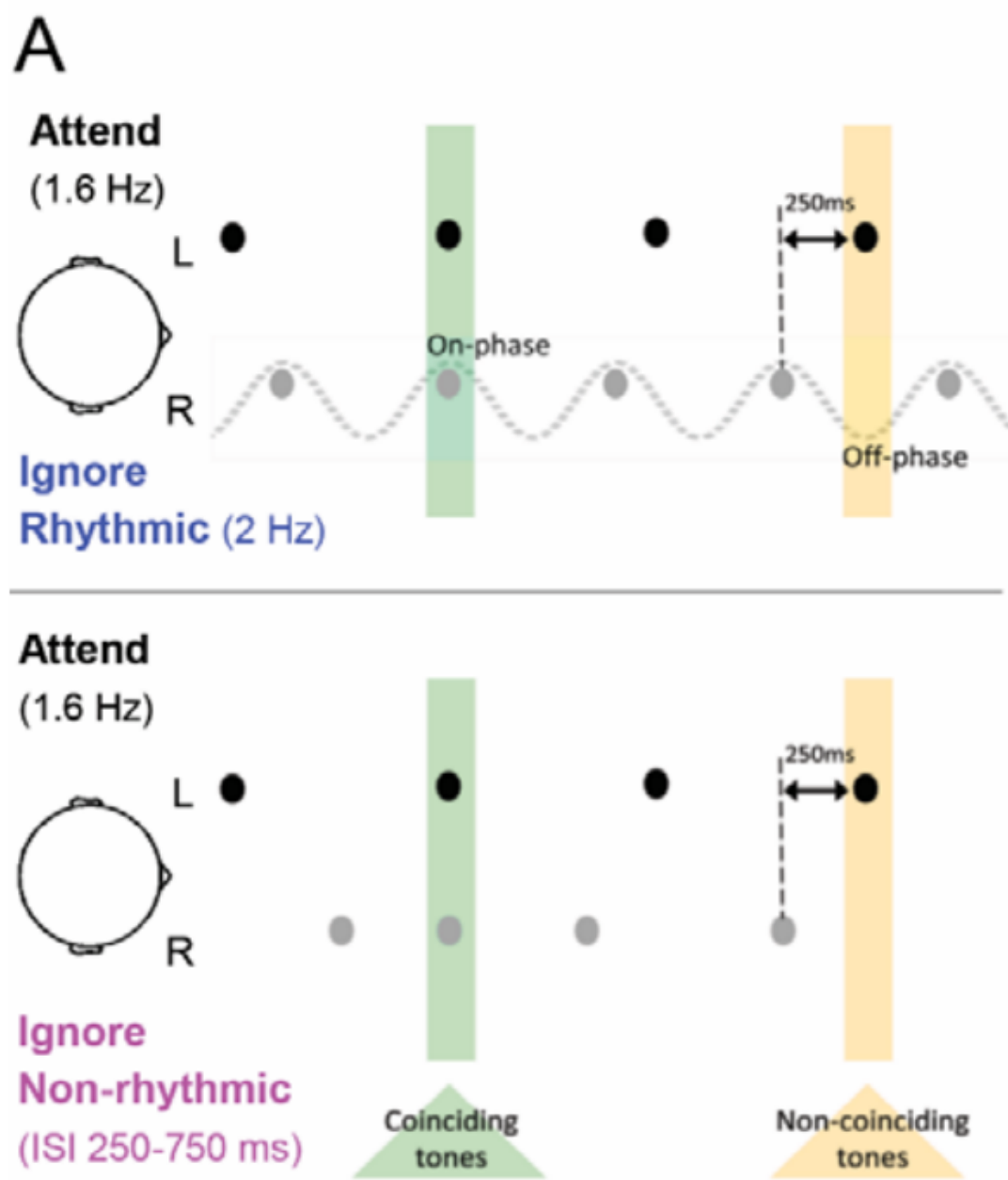
Current Biology

- B) Psychometric functions. The horizontal axis shows the face morphing level. Positive values indicate female faces (lighter shades), and negative values stand for male faces (dark shades). The vertical axis indicates the proportion of female responses. Colored curves show the logistic fits to the psychometric results for the eight tested locations separately. The angular location of the eight locations are color coded (angles begin at 0° to the right of the fixation and increase in the counterclockwise direction). Actual data points are shown only for the leftmost and rightmost curves to avoid visual clutter. The two gray arrows indicate points of subjective equality (PSEs) of the most female-biased (left) and the most male-biased (right) curves.

Markov 2020-

BioRxiv

A



- Experimental design and behavioral results. (A) The temporal relation between sounds in the to-be-attended (left ear, black dots) and to-be-ignored (right ear, gray dots) streams. The to-be-attended stream consisted of an oddball sequence of tones presented at a fixed rate of 1.6 Hz (SOA 625 ms; 500 Hz standards, slightly above threshold pitch deviants). The to-be-ignored (distractor) stream consisted of a sequence of 680 Hz pure tones that was either Rhythmic (top; 2 Hz, SOA 500 ms) or Non-rhythmic (bottom; SOA 250- 750 ms). The temporal relations between the attended (black) and ignored (gray) tones were controlled such that in both distraction conditions 25% of the attended tones coincided with a distractor tone ("coinciding tones", green) and 25% appeared 250 ms following a distractor ("non-coinciding attended tones", yellow). Target sounds occurred only at these positions, ensuring control of low-level acoustics between the Rhythmic and Non-rhythmic Distraction conditions.

Markov 2020-

BioRxiv

- Data Analysis – Behavior Responses to target-tones occurring within a window of 150-1250 ms after target onset were considered “hits”. All other responses were considered false alarms (FAs). Reaction times (RTs) were assessed only for “hit” responses. To test the accuracy and RT measures, we fitted generalized linear mixed effects models, implemented in the statistics software R using the lme4 (Bates et al. 2015) and lmerTest (Kuznetsova et al. 2017) packages. For fitting accuracy rates we used a logit link function, with p-values based on asymptotic Wald tests that are provided in the summary of R's glmer function. For the RT model, p- values were obtained using the Satterthwaite's degrees of freedom approximation (Satterthwaite 1946). All models converged with a maximal random structure, as random intercepts and slopes of all predictors were included, adjusted by subjects.

Markov 2020-

BioRxiv

- For each behavioral measure (accuracy and RT) we fitted a model to test the overall performance, using the Temporal Structure of the distractor as predictor. This predictor was Helmert coded: one beta codes for the contrast between the No-distraction condition and the average in the two Distraction conditions, and the second beta codes for the contrast between The Rhythmic and Non-Rhythmic distraction conditions.

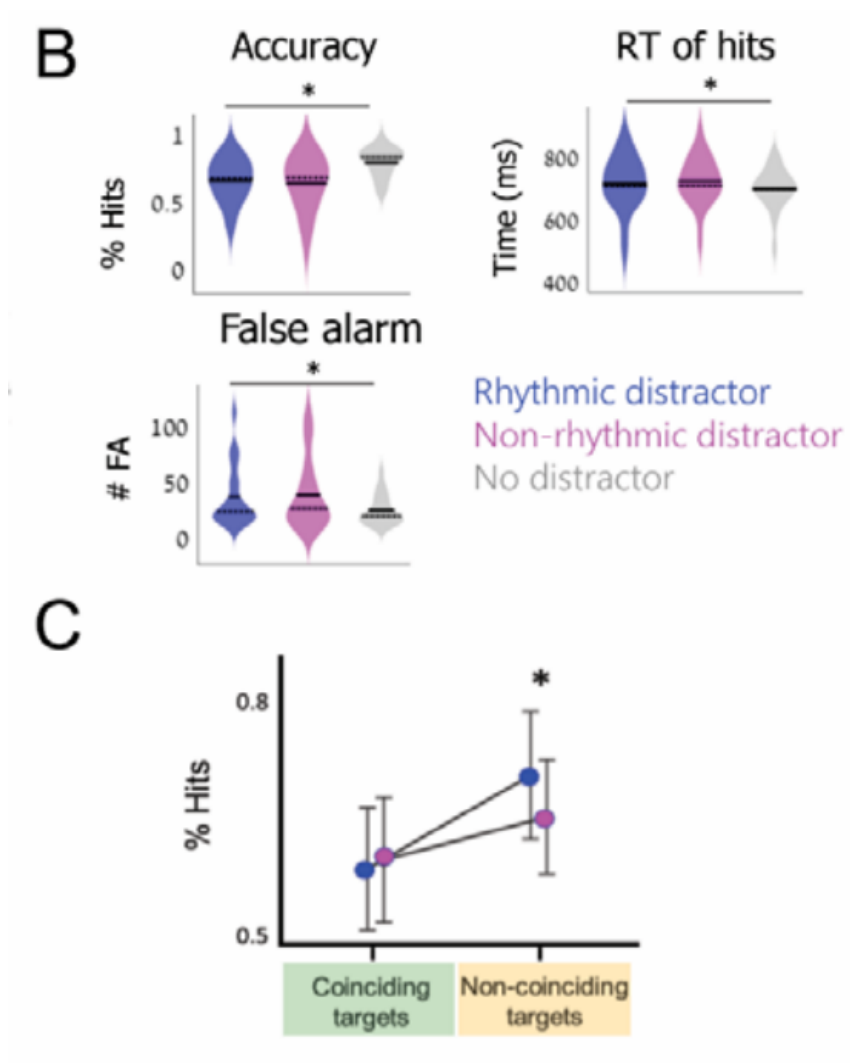
Markov 2020-

BioRxiv

- We then applied a second model on the hit-rates data, to explore the interaction between the distractors' Temporal Structure (Rhythmic vs. Non- rhythmic) and the Temporal Coincidence of targets and distractor tones (Coinciding vs. Non-coinciding), using both variables and their interaction as predictors. Variables were sum coded, i.e. each beta reflects the difference from the grand mean. The non-balanced number of “hits” in each category precluded similar analysis of RTs. The measure of FA rates included only one value per condition for each subject, and thus was statistically assessed via permutation tests, contrasting (a) No-distraction vs. both Distraction conditions and (b) Rhythmic vs. Non- rhythmic distraction.

Markov 2020-

BioRxiv



- (B) Accuracy, False alarm rates and RT in response to targets appearing in the presence of Rhythmic (blue), Non-rhythmic (pink) or No distraction (gray). In each violin plot (Hoffmann 2015), the full and dashed horizontal lines denote the mean and median, respectively. All behavioral measures indicate that both distraction types were disruptive for task performance.
- (C) Modulation of target-detection accuracy by Distraction Type (Rhythmic vs. Non-rhythmic) and Temporal Coincidence between the streams (Coinciding vs. Non-coinciding). Accuracy was improved for targets occurring 250 ms after a distractor tone in the Rhythmic condition (namely, at the off-phase of the distractor rhythm).